AIMS Mathematics, 11(3): 6030–6049.
DOI: 10.3934/math.2026250
Received: 08 December 2025
Revised: 18 February 2026
Accepted: 03 March 2026
Published: 10 March 2026

https://www.aimspress.com/journal/Math

Research article

Computation of the eigenvalues of a second-order boundary value problem with parameter dependent boundary conditions

Ayşe Kabataş[1] **and Süleyman Şengül**[2,*]

[1] Department of Mathematics, Faculty of Science, Karadeniz Technical University, Trabzon 61080, Türkiye

[2] Department of Mathematics, Faculty of Arts and Sciences, Recep Tayyip Erdoğan University, Rize 53100, Türkiye

* **Correspondence:** Email: suleyman.sengul@erdogan.edu.tr.

Abstract: Our purpose in this paper was to determine the eigenvalues of the boundary value problem with separated and parameter dependent boundary conditions when the potential function is integrable and symmetric. We first provided the asymptotic estimates of the eigenvalues of the related problem. Second, we computed numerical results for the eigenvalues using the interpolating element free Galerkin method. Then, a few examples are presented to illustrate the power of the method and compare the asymptotical and numerical results for consistency and validity.

Keywords: boundary value problems; eigenvalues; asymptotic approximation; interpolating element free Galerkin method
Mathematics Subject Classification:34B09, 34B30, 34L15

1. Introduction

We consider the following second-order boundary value problem with the differential equation

$$y''(x) + [\lambda^2 - q(x)]y(x) = 0 \tag{1.1}$$

and the separated boundary conditions

$$y(0)\cos\alpha + y'(0)\sin\alpha = 0, \tag{1.2}$$

$$y(a)\cos\beta + y'(a)\sin\beta + f(\lambda)[y(a)\cos\gamma + y'(a)\sin\gamma] = 0 \tag{1.3}$$

where λ is a real spectral parameter, $q(x)$ is a real-valued and integrable on $[0, a]$, $f(\lambda)$ is an odd real entire function of λ of order less than 1, and $\sin(\beta - \gamma) \neq 0$ ($\alpha, \beta, \gamma \in (0, \pi)$). Also, without loss of generality, we assume $\int_0^a q(t)dt = 0$.

Second-order eigenvalue problems appear frequently throughout applied mathematics. In recent years, there has been a notable resurgence of interest in these problems, from a mathematical standpoint and because of their applications in physics and engineering [5]. Many significant problems in science and engineering require the determination of the eigenvalues and their associated eigenfunctions [3,4,15,18]. The general theory of eigenvalues and eigenfunctions represents one of the most profound and extensive areas within mathematical physics [6, 25, 26]. In practical applications, such as those concerning the vibration and stability of deformable structures, the most critical piece of information is often the smallest eigenvalue [9, 19]. Engineers commonly focus on the smallest eigenvalue because it tends to reveal essential characteristics of dynamic systems. Structural damage caused by seismic activity can be devastating if the fundamental frequency of the structure (which is related to the smallest eigenvalue) is close to the frequency of the earthquake [9]. Eigenvalues also play a key role in determining the stability region of solutions to second-order eigenvalue problems [7]. In general, computing the eigenvalues and their corresponding nontrivial solutions remains a challenging task.

Boundary value problems with parameter-dependent boundary conditions have gained considerable importance in mathematical physics and mechanics [17, 23, 24]. It is well known that eigenvalue problems with eigenparameter dependent boundary conditions are obtained by separating variables in partial differential equations such as wave mechanics and thermodynamics [20]. Eigenvalue problems like

$$\left.\begin{array}{c} y''(x) + [\lambda - q(x)]y(x) = 0, \quad a \le x \le b \\ P(\lambda)y(a) + Q(\lambda)y'(a) = 0, \\ R(\lambda)y(b) + S(\lambda)y'(b) = 0 \end{array}\right\} \tag{1.4}$$

were studied by many researches, where P, Q, R, S have linearly dependence on parameter λ. The wide application of such problems in mechanics, physics, and engineering has stimulated people's interest in research [2, 16]. Fulton [20] first studied the asymptotic formulae for eigenvalues of the two-point boundary value problems involving the eigenvalue parameter in the boundary condition at the one endpoint. In this work, physical applications of such problems are found.

The boundary value problems that interest us in this paper are those where boundary conditions in (1.4) are replaced by

$$\left.\begin{array}{c} y''(x) + [\lambda - q(x)]y(x) = 0, \quad a \le x \le b \\ \tilde{P}(\sqrt{\lambda})y(a) + \tilde{Q}(\sqrt{\lambda})y'(a) = 0, \\ \tilde{R}(\sqrt{\lambda})y(b) + \tilde{S}(\sqrt{\lambda})y'(b) = 0 \end{array}\right\} \tag{1.5}$$

where $\tilde{P}, \tilde{Q}, \tilde{R}$, and $\tilde{S}$ are polynomials. Problems of these types have been studied by a few researchers such as Benedek and Panzone [8], Hochstadt [22], and Kerimov and Mamedov [27] for $\tilde{P}, \tilde{Q}, \tilde{R}$, and $\tilde{S}$ are linear. Problem (1.1)–(1.3) is a particular case of (1.5).

Several researchers have combined analytical and numerical techniques to investigate classes of partial differential equations, particularly subdiffusion and nonlinear evolution equations [37, 38]. Many of these problems involve spatial differential operators that can be formulated within the second-order eigenvalue problem framework. The spectral properties of such operators play a fundamental role in stability analysis, error estimation, and structure-preserving discretization schemes [35, 36]. Motivated by these developments,we focus on the eigenvalue structure of the problem defined in (1.1)–(1.3), providing theoretical insights that may also support the analysis of numerical schemes.

The eigenvalues of the problem (1.1)–(1.3) generally cannot be obtained by analytical methods. In such cases, the eigenvalues are determined by asymptotic or numerical approaches. When the boundary conditions do not depend on the eigenvalue parameter, the eigenvalues of Sturm–Liouville problems are computed numerically by many methods [1, 10, 12]. However, when the boundary conditions depend on the eigenvalue parameter, the number of available numerical studies is limited. Tharwat et al. [32, 33] computed the numerical eigenvalues of Sturm–Liouville problems with an internal point of discontinuity using the sinc method based on the sampling theory and the sinc–Gauss method. Chanane [13, 14] calculated the eigenvalues of Sturm–Liouville problems with nonlinear boundary conditions and non-self-adjoint Sturm–Liouville problems by means of the regularized sampling method. Mukhtarov and Yücel [29] obtained the eigenvalues and eigenvectors of singular Sturm–Liouville problems using the Adomian decomposition method.

Meshless methods are among the popular techniques commonly used for the numerical solution of differential equations. In these methods, it is not necessary to construct a mesh between the nodes. Only the locations of the nodes are specified, and the shape functions are constructed as part of the solution procedure. However, studies on the determination of eigenvalues or eigenfunctions of Sturm–Liouville problems using meshless methods remain relatively limited. Shen [31] determined the eigenvalues of Sturm–Liouville problems with boundary conditions by employing a local radial basis function-based differential quadrature (LRBFDQ) collocation method. Reutskiy [30] computed the eigenvalues of generalized Sturm–Liouville problems, in which the boundary conditions depend on the eigenvalue parameter, using the asymmetric radial basis function (RBF) collocation method. Baskaya and Sengul [6] calculated the eigenvalues of Sturm–Liouville problems with integrable and symmetric potentials by means of the element-free Galerkin method.

The limited number of such studies, together with the fact that mesh generation between nodes is not required, enhances the applicability of meshless methods to Sturm–Liouville problems. In this study, we obtain numerical results by employing the interpolating element-free Galerkin method to analyze the accuracy of asymptotic results, thereby adopting an approach that differs from those available in the literature. Since the shape functions in this method satisfy the Kronecker delta property, Dirichlet boundary conditions can be imposed directly without requiring any additional techniques. In contrast, in the standard element-free Galerkin method, extra procedures such as the penalty method or Lagrange multipliers are needed to enforce Dirichlet boundary conditions.

Our purpose of this paper is twofold. First, we derive novel asymptotic estimates for the eigenvalues of the problem (1.1)–(1.3) when the potential function is integrable and symmetric on the finite interval $[0, a]$. The symmetry of the potential is of particular importance in quantum mechanics, since it enables the reduction of the problem to a half-interval formulation. Second, we compute the eigenvalues of the related problem numerically by employing the interpolating element-free Galerkin (IEFG) method. The numerical results are used to confirm the validity and sharpness of the asymptotic estimates derived in this study, which are obtained here for the first time.

2. Asymptotic estimates

2.1. Method

In this section, to determine the asymptotic estimates for the eigenvalues of (1.1)–(1.3), we use a similar approach to Harris [21]. According to this, we assume that $y(x, \lambda)$ is a complex-valued solution

of (1.1) and apply the transform $v(x,\lambda) = y'(x,\lambda)/y(x,\lambda)$ to the equation (1.1). This gives the Riccati equation

$$v' = -\lambda^2 + q - v^2. \tag{2.1}$$

Let $v(x,\lambda)$ be a complex-valued solution of (2.1) and define

$$S(x,\lambda) := Re\{v(x,\lambda)\}, \tag{2.2}$$
$$T(x,\lambda) := Im\{v(x,\lambda)\}. \tag{2.3}$$

Then any nontrivial real-valued solution of (1.1) may be written as

$$y(x,\lambda) = R(x,\lambda)\cos(\Psi(x,\lambda)), \tag{2.4}$$

where

$$\frac{R'}{R} = S(x,\lambda), \quad \Psi' = T(x,\lambda). \tag{2.5}$$

Our approach to approximating the eigenvalues λ_n of (1.1)-(1.2) is to approximate those λ, which are

$$\Psi(a,\lambda) - \Psi(0,\lambda) = \int_0^a T(t,\lambda)dt. \tag{2.6}$$

We suppose that there exist functions $A(x)$ and $\eta(\lambda)$, so that

$$\left|\int_x^a e^{2i\lambda t}q(t)dt\right| \le A(x)\eta(\lambda),$$

where

(i) $A(x) := \int_x^a |q(t)|\,dt$ is a decreasing function of x,
(ii) $A(x) \in L^1[0,\pi]$,
(iii) $\eta(\lambda) \to 0$ as $\lambda \to \infty$.

For $q \in L[0,a]$, the existence of the A and η functions may be established for λ positive as follows: We note that, avoiding the trivial case $\int_x^a |q(t)|\,dt = 0$,

$$\left|\int_x^a e^{2i\lambda t}q(t)dt\right| \le \int_x^a |q(t)|\,dt < \infty.$$

Thus, if we define

$$F(x,\lambda) := \begin{cases} |\int_x^a e^{2i\lambda t}q(t)dt| / \int_x^a |q(t)|dt, & if \int_x^a |q(t)|dt \neq 0 \\ 0, & if \int_x^a |q(t)|dt = 0, \end{cases} \tag{2.7}$$

then $0 \le F(x,\lambda) \le a$, and we set $\eta(\lambda) := sup_{0\le x\le a}F(x,\lambda)$. Note that $\eta(\lambda)$ is well-defined by (2.7) and $\eta(\lambda) \to 0$ as $\lambda \to \infty$ [21]. We now approximate to a solution of (2.1) on $[0,a]$ and set

$$v(x,\lambda) := i\lambda + \sum_{n=1}^{\infty} v_n(x,\lambda). \tag{2.8}$$

We put this serie into the Riccati equation (2.1) and choose v_n so that

$$v_1' + 2i\lambda v_1 = q,$$
$$v_2' + 2i\lambda v_2 = -v_1^2,$$

and for $n = 3, 4, ...,$

$$v_n' + 2i\lambda v_n = -(v_{n-1}^2 + 2v_{n-1}\sum_{m=1}^{n-2} v_m).$$

By solving these first-order linear differential equations, we have v_ns, such that

$$v_1(x,\lambda) = -e^{-2i\lambda x}\int_x^a e^{2i\lambda t}q(t)dt, \tag{2.9}$$

$$v_2(x,\lambda) = e^{-2i\lambda x}\int_x^a e^{2i\lambda t}v_1^2(t,\lambda)dt, \tag{2.10}$$

and

$$v_n(x,\lambda) = e^{-2i\lambda x}\int_x^a e^{2i\lambda t}[v_{n-1}^2(t,\lambda) + 2v_{n-1}(t,\lambda)\sum_{m=1}^{n-2} v_m(t,\lambda)]dt, \quad n \geq 3. \tag{2.11}$$

It is shown in [21] that $\sum_{n=1}^{\infty} v_n(x,\lambda)$ is uniformly absolutely convergent for all $\lambda \geq \lambda_0$ and for all $x \in [0,a]$. It also follows from the choice of v_ns that $\sum_{n=1}^{\infty} v_n'(x,\lambda)$ is uniformly absolutely convergent. The series $i\lambda + \sum_{n=1}^{\infty} v_n(x,\lambda)$ is therefore a solution of (2.1). Hence, from (2.2), (2.3), and (2.8), we can write

$$S(x,\lambda) = Re\{v(x,\lambda)\} = Re\left(\sum_{n=1}^{\infty} v_n(x,\lambda)\right), \tag{2.12}$$

$$T(x,\lambda) = Im\{v(x,\lambda)\} = \lambda + Im\left(\sum_{n=1}^{\infty} v_n(x,\lambda)\right). \tag{2.13}$$

By the definition of $\eta(\lambda)$ in (2.7), equation (2.8) gives as $\lambda \to \infty$

$$v(x,\lambda) = i\lambda + v_1(x,\lambda) + O(\eta^2(\lambda)), \tag{2.14}$$

where

$$\begin{aligned} v_1(x,\lambda) =& -e^{-2i\lambda x}\int_x^a e^{2i\lambda t}q(t)dt \\ =& [i\sin(2\lambda x) - \cos(2\lambda x)]\int_x^a q(t)[\cos(2\lambda t) + i\sin(2\lambda t)]dt. \end{aligned} \tag{2.15}$$

Thus, substituting (2.14) and (2.15) into (2.12) gives

$$S(x,\lambda) = -(\cos(2\lambda x))\int_x^a q(t)\cos(2\lambda t)dt - (\sin(2\lambda x))\int_x^a q(t)\sin(2\lambda t)dt + O(\eta^2(\lambda)).$$

Let us define the following notations to abbreviate:

$$\sin\xi_x := \int_x^a q(t)\cos(2\lambda t)dt, \quad \cos\xi_x := \int_x^a q(t)\sin(2\lambda t)dt.$$

Thus, we can write $S(x,\lambda)$ as

$$S(x,\lambda) = -\sin(2\lambda x + \xi_x) + O(\eta^2(\lambda)). \tag{2.16}$$

Similarly, by using (2.14) and (2.15) into (2.13), $T(x,\lambda)$ is presented as

$$T(x,\lambda) = \lambda - \cos(2\lambda x + \xi_x) + O(\eta^2(\lambda)). \tag{2.17}$$

Also, by a change in the order of integration we gain, respectively,

$$\int_0^a v_1(t,\lambda)dt = \frac{-i}{2\lambda}\int_0^a q(t)(1-e^{2i\lambda t})dt = \frac{i}{2\lambda}\int_0^a q(t)e^{2i\lambda t}dt, \tag{2.18}$$

$$\int_0^a v_2(t,\lambda)dt = \frac{i}{2\lambda}\int_0^a v_1^2(t,\lambda)\left[1-e^{2i\lambda t}\right]dt \tag{2.19}$$

and

$$\int_0^a v_n(t,\lambda)dt = \frac{i}{2\lambda}\int_0^a \left[v_{n-1}^2(t,\lambda) + 2v_{n-1}(t,\lambda)\sum_{m=1}^{n-2} v_m(t,\lambda)\right]\left[1-e^{2i\lambda t}\right]dt, \quad n \geq 3. \tag{2.20}$$

2.2. Results

In this section, we obtain asymptotic formulas for λ_n and the eigenvalues of the problem (1.1)–(1.3), within an error term of arbitrary order under the condition that the potential function $q(x)$ is a real-valued function that is integrable and symmetric on the finite interval $[0,a]$. Hochstadt in [22] used this problem for the inverse approach and took $f(\lambda) = c\lambda$, $c \neq 0$. We also use this value of $f(\lambda)$ for the calculation. The other cases can be treated similarly.

Theorem 1. *The eigenvalues λ_n of (1.1)–(1.3) satisfy as $\lambda \to \infty$*

$$\begin{aligned}(n+1)\pi =& \lambda a + \sum_{n=1}^{\infty} Im\left\{\int_0^a v_n(t,\lambda)dt\right\} + tan^{-1}\left[\frac{\cos\alpha + S(0,\lambda)\sin\alpha}{T(0,\lambda)\sin\alpha}\right] \\ & - tan^{-1}\left[\frac{\cos\beta + c\lambda\cos\gamma + S(a,\lambda)(\sin\beta + c\lambda\sin\gamma)}{T(a,\lambda)(\sin\beta + c\lambda\sin\gamma)}\right].\end{aligned} \tag{2.21}$$

Proof. From (2.4), we have

$$\begin{aligned}y(0)\cos\alpha + y'(0)\sin\alpha =& R(0,\lambda)\cos(\Psi(0,\lambda))\cos\alpha + R'(0,\lambda)\cos(\Psi(0,\lambda))\sin\alpha \\ & - R(0,\lambda)\Psi'(0,\lambda)\sin(\Psi(0,\lambda))\sin\alpha \\ =& R(0,\lambda)\sin(\Psi(0,\lambda) + A)\end{aligned} \tag{2.22}$$

where

$$\sin A := \cos\alpha + \frac{R'(0,\lambda)}{R(0,\lambda)}\sin\alpha \quad \text{and} \quad \cos A := -\Psi'(0,\lambda)\sin\alpha. \tag{2.23}$$

Hence, using (2.5) and (2.23), we find that

$$A = -tan^{-1}\left[\frac{\cos\alpha + S(0,\lambda)\sin\alpha}{T(0,\lambda)\sin\alpha}\right]. \tag{2.24}$$

Thus, by considering (1.2) and (2.22), we obtain

$$\Psi(0,\lambda) = -A = tan^{-1}\left[\frac{\cos\alpha + S(0,\lambda)\sin\alpha}{T(0,\lambda)\sin\alpha}\right]. \tag{2.25}$$

Similarly, the second boundary condition (1.3) is satisfied if

$$\Psi(a,\lambda) = (n+1)\pi + tan^{-1}\left[\frac{\cos\beta + c\lambda\cos\gamma + S(a,\lambda)(\sin\beta + c\lambda\sin\gamma)}{T(a,\lambda)(\sin\beta + c\lambda\sin\gamma)}\right] \tag{2.26}$$

for the integer n. The result (2.21) now follows from (2.6), (2.13), (2.25), and (2.26). □

Theorem 2. *The eigenvalues λ_n of the problem (1.1)–(1.3) satisfy*

$$\begin{aligned}\lambda_n =& \frac{(n+1)\pi}{a} + \frac{a}{(n+1)\pi}[\cot\gamma - \cot\alpha + \frac{1}{2}\int_0^a q(t)\cos\left(\frac{2(n+1)\pi t}{a}\right)dt] \\ &+ O(n^{-1}\eta^2(n)) + O(n^{-2}\eta(n)), \quad n \to \infty.\end{aligned} \tag{2.27}$$

Proof. Similar to [6], using (2.18)–(2.20), it is shown that

$$\begin{aligned}\int_0^a \sum_{n=1}^{\infty} Im\{v_n(t,\lambda)\}\,dt &= \sum_{n=1}^{\infty} Im\left\{\int_0^a v_n(t,\lambda)dt\right\} \\ &= \frac{1}{2}\lambda^{-1}\int_0^a q(t)\cos(2\lambda t)dt + O(\lambda^{-2}\eta(\lambda)).\end{aligned} \tag{2.28}$$

Now, we calculate $\tan A$ from (2.23) using (2.5), (2.16), and (2.17), so that

$$\begin{aligned}\tan A =& -\frac{\cos\alpha + S(0,\lambda)\sin\alpha}{T(0,\lambda)\sin\alpha} \\ =& \frac{\cos\alpha - \sin\alpha\sin\xi_0 + O(\eta^2(\lambda))}{-\lambda\sin\alpha\left[1 - \lambda^{-1}\cos\xi_0 + O(\lambda^{-1}\eta^2(\lambda))\right]} \\ =& \left[-\lambda^{-1}\cot\alpha + \lambda^{-1}\sin\xi_0 + O(\lambda^{-1}\eta^2(\lambda))\right]\left[1 + \lambda^{-1}\cos\xi_0 + O(\lambda^{-1}\eta^2(\lambda))\right] \\ =& -\lambda^{-1}\cot\alpha + \lambda^{-1}\sin\xi_0 + O(\lambda^{-1}\eta^2(\lambda)).\end{aligned}$$

With the last equation, one obtains

$$A = -\lambda^{-1}\cot\alpha + \lambda^{-1}\sin\xi_0 + O(\lambda^{-1}\eta^2(\lambda)). \tag{2.29}$$

Similarly, we take into account (2.26). In this manner, using (2.16) and (2.17) gives

$$\begin{aligned}
&\frac{\cos\beta + c\lambda\cos\gamma + S(a,\lambda)(\sin\beta + c\lambda\sin\gamma)}{T(a,\lambda)(\sin\beta + c\lambda\sin\gamma)} \\
&= \frac{\cos\beta + c\lambda\cos\gamma + O(\eta^2(\lambda)) + O(\lambda\eta^2(\lambda)))}{[\lambda + O(\eta^2(\lambda))][\sin\beta + c\lambda\sin\gamma]} \\
&= \frac{\cos\beta + c\lambda\cos\gamma + O(\lambda\eta^2(\lambda)))}{c\lambda^2\sin\gamma\left[1 + \lambda^{-1}\dfrac{\sin\beta}{c\sin\gamma} + O(\lambda^{-1}\eta^2(\lambda))\right]} \\
&= \left[\lambda^{-1}\cot\gamma + O(\lambda^{-1}\eta^2(\lambda))\right]\left[1 - \lambda^{-1}\frac{\sin\beta}{c\sin\gamma} + O(\lambda^{-1}\eta^2(\lambda))\right] \\
&= \lambda^{-1}\cot\gamma + O(\lambda^{-1}\eta^2(\lambda)). \qquad (2.30)
\end{aligned}$$

From (2.6), (2.25), (2.26), (2.28), (2.29), and (2.30), we gain

$$\begin{aligned}
(n+1)\pi + \lambda^{-1}\left[\cot\gamma - \cot\alpha\right] + \lambda^{-1}\sin\xi_0 + O(\lambda^{-1}\eta^2(\lambda)) \\
= \lambda a + \frac{1}{2}\lambda^{-1}\sin\xi_0 + O(\lambda^{-2}\eta(\lambda)).
\end{aligned}$$

Finally, we prove the result given by (2.27) using the definition of $\eta(\lambda)$ and series error computation in the last equation. □

Corollary 3. *The eigenvalues λ_n of the problem (1.1)–(1.3) with symmetric potential satisfy*

$$\begin{aligned}
\lambda_n =& \frac{(n+1)\pi}{a} + \frac{a}{(n+1)\pi}[\cot\gamma - \cot\alpha + \int_0^{a/2} q(t)\cos\left(\frac{2(n+1)\pi t}{a}\right)dt] \\
&+ O(n^{-1}\eta^2(n)) + O(n^{-2}\eta(n)), \quad n \to \infty. \qquad (2.31)
\end{aligned}$$

Proof. To prove the corollary, let us calculate the following integral using symmetric potential, i.e., $q(x) = q(a-x)$:

$$\begin{aligned}
\int_{a/2}^{a} q(t)\cos\left(\frac{2(n+1)\pi t}{a}\right)dt &= \int_{a/2}^{a} q(a-t)\cos\left(\frac{2(n+1)\pi t}{a}\right)dt \\
&= -\int_{a/2}^{0} q(u)\cos\left(\frac{2(n+1)\pi(a-u)}{a}\right)du \\
&= \int_0^{a/2} q(u)\cos\left(2(n+1)\pi - \frac{2(n+1)\pi u}{a}\right)du \\
&= \int_0^{a/2} q(t)\cos\left(\frac{2(n+1)\pi t}{a}\right)dt.
\end{aligned}$$

This confirms

$$\int_0^{a} q(t)\cos\left(\frac{2(n+1)\pi t}{a}\right)dt = 2\int_0^{a/2} q(t)\cos\left(\frac{2(n+1)\pi t}{a}\right)dt.$$

Substitution of the last equality into (2.27) proves the corollary (4.2). □

3. Numerical method

3.1. The Interpolating moving least squares method

In Section 2.2, the asymptotic results of the boundary value problem (1.1)–(1.3) were obtained. In this section, a numerical results is proposed for comparison with the asymptotic results. The numerical method employed in this study is the interpolating element-free Galerkin (IEFG) method [11], which is the meshfree method. In the IEFG method, the interpolating moving least squares (IMLS) [28] approach is employed to construct the shape functions.

Let $y^h(x)$ denote the approximation function for the solution $y(x)$ of the problem (1.1)–(1.3). Let $X = \{x_1, x_2, ..., x_N\}$ represent the set of nodes selected in the domain of the problem, $\Omega = [0, a]$, where N is the number of nodes. Furthermore, let $p_0(x) \equiv 1$, $p_1(x)$, ..., $p_m(x)$ denote the given basis functions, where $m + 1$ represents the number of basis functions. In the IMLS method, the new basis functions are defined using these original basis functions. The first basis function is obtained by normalizing the basis function $p_0(x)$

$$\tilde{p}_0(x; \bar{x}) = \frac{p_0(x)}{\|p_0(x)\|_x}. \tag{3.1}$$

Here, the inner product is denoted by

$$(f, g)_x = \sum_{i=1}^{N} w(x, x_i) f(x_i) g(x_i) \tag{3.2}$$

and the norm associated with this inner product is denoted by

$$\|f\|_x = \left[\sum_{i=1}^{N} w(x, x_i) f^2(x_i) \right]^{1/2}. \tag{3.3}$$

In equation (3.2), the subscript x denotes a point in the problem domain Ω and $w(x, x_i)$ represents the weight function associated with the node x_i. In this study, the weight function $w(x, x_i)$ is defined as follows:

$$w(x, x_i) = \begin{cases} \|\frac{x - x_i}{\rho_i}\|^{-\alpha}, & \|x - x_i\| \le \rho_i \\ 0, & others. \end{cases} \tag{3.4}$$

Here, ρ_i denotes the radius of the influence domain associated with the node x_i, $i = 1, 2, ..., N$, parameter α is an even positive integer, and $\|\cdot\|$ represents the Euclidean norm [34]. Thus, the influence domain of x_i can be expressed as

$$\Omega_i = \{x | \, \|x - x_i\| \le \rho_i, x \in \Omega\}.$$

From the definition of the weight functions w, for any point x, only the weight functions whose influence domains contain this point will have nonzero values. Therefore, for a given $x \in \Omega$, the set of indices of the weight functions whose influence domains include this point can be denoted by

$$\tau_x = \{I | \, \|x - x_I\| \le \rho_I, x_I \in X\}.$$

With these definitions, the basis function $\tilde{p}_0(x;\bar{x})$ in equation (3.1) is obtained as

$$\tilde{p}_0(x;\bar{x}) = \frac{1}{\left[\sum_{I\in\tau_x} w(x,x_I)\right]^{1/2}}. \tag{3.5}$$

The remaining basis functions are constructed to be orthogonal to the basis function $\tilde{p}_0(x;\bar{x})$

$$\tilde{p}_i(x;\bar{x}) = p_i(\bar{x}) - S\,p_i(x), \quad i = 1,2,...,m. \tag{3.6}$$

Here, S is a linear operator defined as

$$S\,p_i(x) = \sum_{I\in\tau_x} v(x,x_I)p_i(x_I), \tag{3.7}$$

and

$$v(x,x_I) = \frac{w(x,x_I)}{\sum_{J\in\tau_x} w(x,x_J)}. \tag{3.8}$$

Using the newly defined basis functions, the local approximation function $y^h(x)$ is defined as

$$y^h(x,\bar{x}) = \tilde{p}_0(x;\bar{x})a_0(x) + \sum_{i=1}^{m} \tilde{p}_i(x;\bar{x})a_i(x). \tag{3.9}$$

where $\bar{x}$ is a point within the influence domain of x, and $a_i(x)$, $i = 0,1,...,m$ are the unknown functions.

In the IMLS method, for a given point x, the unknown functions are determined by minimizing the weighted discrete L_2 norm of the difference between the local approximation function $y^h(x,\bar{x})$ and the function $y(\bar{x})$

$$min\ J = \|y^h(x,\cdot) - y(\cdot)\|_x^2 = \sum_{I\in\tau_x} w(x,x_I)[y^h(x,x_I) - y_I]^2, \tag{3.10}$$

or, equivalently

$$(y(\cdot) - y^h(x,\cdot), \tilde{p}_0)_x = 0, \tag{3.11}$$

$$(y(\cdot) - y^h(x,\cdot), \tilde{p}_i)_x = 0, \quad i = 1,2,...,m. \tag{3.12}$$

Here, $y_i = y(x_i)$ is called the nodal parameter. By utilizing the properties of the inner product, it is obtained that

$$a_0(x) = (y, \tilde{p}_0)_x \tag{3.13}$$

and

$$\sum_{i=1}^{m} a_i(x)(\tilde{p}_i, \tilde{p}_j)_x = (y - S\,y, \tilde{p}_j)_x, \quad j = 1,2,...,m \tag{3.14}$$

where $S\,y = \sum_{I\in\tau_x} v(x,x_I)y_I$. Because of $(S\,y, \tilde{p}_i)_x = 0, i = 1,2,...,m$ [34], equation (3.14) is written as

$$\sum_{i=1}^{m} a_i(x)(\tilde{p}_i, \tilde{p}_j)_x = (y, \tilde{p}_j)_x, \quad j = 1,2,...,m. \tag{3.15}$$

(3.15) can be expressed in matrix form as

$$\mathbf{A}(x)\mathbf{a}(x) = \mathbf{F}_w(x)\mathbf{y}. \tag{3.16}$$

Here,

$$\mathbf{a}^T(x) = (a_1(x), a_2(x), \cdots, a_m(x))$$
$$\mathbf{y}^T = (y_1, y_2, \cdots, y_N)$$
$$\mathbf{A}(x) = \mathbf{F}_w(x)\mathbf{F}^T(x)$$
$$\mathbf{F}(x) = \begin{bmatrix} \tilde{p}_1(x;x_1) & \tilde{p}_1(x;x_2) & \cdots & \tilde{p}_1(x;x_N) \\ \tilde{p}_2(x;x_1) & \tilde{p}_2(x;x_2) & \cdots & \tilde{p}_2(x;x_N) \\ \vdots & \vdots & \vdots & \vdots \\ \tilde{p}_m(x;x_1) & \tilde{p}_m(x;x_2) & \cdots & \tilde{p}_m(x;x_N) \end{bmatrix}$$

and $\mathbf{F}_w(x) = (\bar{w}_{kj}(x))_{mxN}$ is a matrix, where

$$\bar{w}_{kj}(x) = \begin{cases} w(x,x_j)\tilde{p}_k(x;x_j), & x \neq x_j \\ \sum_{I\in\tau_x, I\neq j} w(x_j,x_I)[p_k(x_j) - p_k(x_I)], & x = x_j. \end{cases}$$

Therefore, from (3.16), the unknown vector is obtained as

$$\mathbf{a}(x) = \mathbf{A}^{-1}(x)\mathbf{F}_w(x)\mathbf{y}. \tag{3.17}$$

Consequently, the local approximation is determined from (3.9) as

$$y^h(x,\bar{x}) = Sy + \sum_{i=1}^{m} a_i(x)\tilde{p}_i(x;\bar{x}). \tag{3.18}$$

The global approximation is then obtained as

$$y^h(x) = Sy + \sum_{i=1}^{m} a_i(x)g_i(x) \equiv \Phi(x)\mathbf{y} = \sum_{i=1}^{N} \phi_i(x)y(x_i). \tag{3.19}$$

Here,

$$\Phi(x) = (\phi_1(x), \phi_2(x), \cdots, \phi_N(x)) = \mathbf{v}^T + \mathbf{p}^T(x)\mathbf{A}^{-1}(x)\mathbf{F}_w(x) \tag{3.20}$$

is called a shape function, where

$$\mathbf{v}^T = (v(x,x_1), v(x,x_2), \cdots, v(x,x_N))$$
$$\mathbf{p}^T(x) = (g_1(x), g_2(x), \cdots, g_m(x))$$
$$g_i(x) = p_i(x) - Sp_i(x).$$

The first derivative [34] of the shape function is obtained as

$$\begin{aligned} \Phi_{,i}(x) =& \mathbf{v}_{,i}^T(x) + \mathbf{p}_{,i}^T(x)\mathbf{A}^{-1}(x)\mathbf{F}_w(x) + \mathbf{p}^T(x)\mathbf{A}^{-1}(x)\mathbf{F}_{w,i}(x) \\ &+ \mathbf{p}^T(x)\mathbf{A}_{,i}^{-1}(x)\mathbf{F}_w(x) \end{aligned} \tag{3.21}$$

where

$$\mathbf{F}_{w,i}(x) = (\bar{w}_{kj,i}(x))_{mxN}$$
$$\bar{w}_{kj,i}(x) = \begin{cases} w_{,i}(x,x_j)\tilde{p}_k(x;x_j) + w(x,x_j)\tilde{p}_{k,i}(x;x_j), & x \neq x_j \\ \sum_{I\in\tau_x, I\neq j} w_{,i}(x,x_I)[p_k(x_j) - p_k(x_I)], & x = x_j \end{cases}$$
$$\mathbf{A}_{,i}^{-1}(x) = -\mathbf{A}^{-1}(x)\mathbf{A}_{,i}(x)\mathbf{A}^{-1}(x).$$

3.2. The Interpolating element free Galerkin method

The IEFG method is a meshfree technique developed for the solution of differential equations. In this method, the shape functions are constructed using the IMLS approach. Typically, the weak form of the problem is employed in the solution procedure. Moreover, the weak form is obtained by multiplying both sides of (1.1) by a test function $\mu(x)$ and integrating over the problem domain, which yields

$$\int_0^a y''(x)\mu(x)dx + \int_0^a \left\{\lambda^2 - q(x)\right\} y(x)\mu(x)dx = 0. \tag{3.22}$$

By integration by parts and using the boundary conditions in (1.2) and (1.3), the weak form of problem for $f(\lambda) = c\lambda$ is obtained as

$$\begin{aligned}&\frac{cos(\alpha)}{sin(\alpha)}y(0)\mu(0) - \frac{c\lambda cos(\gamma) + cos(\beta)}{c\lambda sin(\gamma) + sin(\beta)}y(a)\mu(a)\\ &- \int_0^a y'(x)\mu'(x)dx + \int_0^a \left\{\lambda^2 - q(x)\right\} y(x)\mu(x)dx = 0.\end{aligned} \tag{3.23}$$

Substituting the approximation given in (3.19) into the weak form in (3.23) and taking the shape functions as test functions leads to the system of equations

$$\begin{aligned}&\sum_{i=1}^{N}\left[\frac{cos(\alpha)}{sin(\alpha)}\phi_i(0)\phi_j(0) - \frac{c\lambda cos(\gamma) + cos(\beta)}{c\lambda sin(\gamma) + sin(\beta)}\phi_i(a)\phi_j(a)\right]y_i\\ &+ \sum_{i=1}^{N}\left[\int_0^a \left(\lambda^2 - q(x)\right)\phi_i(x)\phi_j(x)dx - \int_0^a \frac{d\phi_i(x)}{dx}\frac{d\phi_j(x)}{dx}dx\right]y_i = 0,\end{aligned} \tag{3.24}$$

$j = 1, 2, ..., N$. If

$$(B_1)_{i,j} := \phi_i(0)\phi_j(0), (B_2)_{i,j} := \phi_i(a)\phi_j(a), M_{i,j} := \int_0^a \frac{d\phi_i(x)}{dx}\frac{d\phi_j(x)}{dx}dx$$

$$K_{i,j} := \int_0^a \phi_i(x)\phi_j(x)dx, C_{i,j} := \int_0^a q(x)\phi_i(x)\phi_j(x)dx, 1 \le i, j \le N,$$

are defined in (3.24), the system equation is found as

$$\left[\frac{cos(\alpha)}{sin(\alpha)}B_1 - \frac{c\lambda cos(\gamma) + cos(\beta)}{c\lambda sin(\gamma) + sin(\beta)}B_2 - M + \lambda^2 K - C\right]Y = 0. \tag{3.25}$$

Therefore, the numerical eigenvalues of (1.1) are determined as the roots of

$$F(\lambda) = \det\left[\frac{cos(\alpha)}{sin(\alpha)}B_1 - \frac{c\lambda cos(\gamma) + cos(\beta)}{c\lambda sin(\gamma) + sin(\beta)}B_2 - M + \lambda^2 K - C\right]. \tag{3.26}$$

To find the roots of the function in the equation (3.26), the Newton-Raphson method is applied in this article.

4. Examples

In this section, we present a few examples to demonstrate the effectiveness of the method and to assess the agreement between the asymptotic and numerical results. For this purpose, the relative error between the numerical eigenvalues obtained using the IEFG and asymptotic approximations of the eigenvalues is evaluated for each n:

$$E_{\text{relative}} = \frac{|\text{numerical eigenvalue using IEFG} - \text{asymptotic eigenvalue}|}{\text{numerical eigenvalue using IEFG}}. \tag{4.1}$$

Example 1.

$$\left.\begin{array}{c} y''(x) + \left[\lambda^2 - |x(1-x)| + \dfrac{1}{6}\right] y(x) = 0, \quad 0 \le x \le 1 \\ y(0) + \sqrt{3}y'(0) = 0, \\ \sqrt{3}y(1) + y'(1) + \lambda\sqrt{2}[y(1) + y'(1)] = 0 \end{array}\right\} \tag{4.2}$$

In our first example, we use the basic symmetric potential function $q(x) = |x(1-x)| - \dfrac{1}{6}$ on the interval $[0, 1]$. This absolute value function is not continuous at the endpoint zero (0); however, it is integrable on the given interval. Additionally, we take $\gamma = \pi/4$, $\alpha = \pi/3$, $\beta = \pi/6$, and $c = 1$ in (1.1)–(1.3), and we have problem (4.2). Thus, using Theorem 2.2, we obtain the asymptotic estimates of the eigenvalues of (4.2) as

$$\lambda_n = (n+1)\pi + \frac{1}{(n+1)\pi}\left[1 - \frac{\sqrt{3}}{3} - \frac{1}{4(n+1)^2\pi^2}\right] + O(n^{-1}\eta^2(n)) + O(n^{-2}\eta(n)). \tag{4.3}$$

If the numerical results are determined using the roots of the function F in (3.26) for $\rho_i = 0.012, N = 100$, Table 1 is obtained.

As shown in Table 1, the asymptotical and numerical approximations are consistent. Moreover, the last column of the table shows that the relative errors are generally small. Except for the first value and for large n, these errors are observed to be on the order of 10^{-4}. Figure 1 shows the relative error plots for the corresponding values of n.

From Figure 1, while the errors for the first three eigenvalues and for large values of n are on the order of 10^{-3}, the errors for the other values of n are approximately on the order of 10^{-4}.

Table 1. Eigenvalue comparison for the symmetric potential $q(x) = |x(1-x)| - \frac{1}{6}$.

n	Asymptotic Appr.	IEFG Appr.	Relative Error (E)
1	6.3494	6.3588	0.0015
2	9.4693	9.4741	0.0005
3	12.5999	12.6028	0.0002
4	15.7348	15.7368	0.0001
5	18.8719	18.8735	0.0001
6	22.0103	22.0118	0.0001
7	25.1495	25.1510	0.0001
8	28.2893	28.2908	0.0001
9	31.4294	31.4312	0.0001
10	34.5697	34.5720	0.0001
11	37.7103	37.7131	0.0001
12	40.8510	40.8545	0.0001
13	43.9919	43.9962	0.0001
14	47.1329	47.1382	0.0001
15	50.2739	50.2805	0.0001
16	53.4150	53.4231	0.0002
17	56.5561	56.5660	0.0002
18	59.6973	59.7093	0.0002
19	62.8386	62.8529	0.0002
20	65.9799	65.9969	0.0003
30	97.3937	97.4631	0.0007
40	128.8086	128.9791	0.0013
50	160.2239	160.4391	0.0013
75	238.7628	238.6293	0.0006

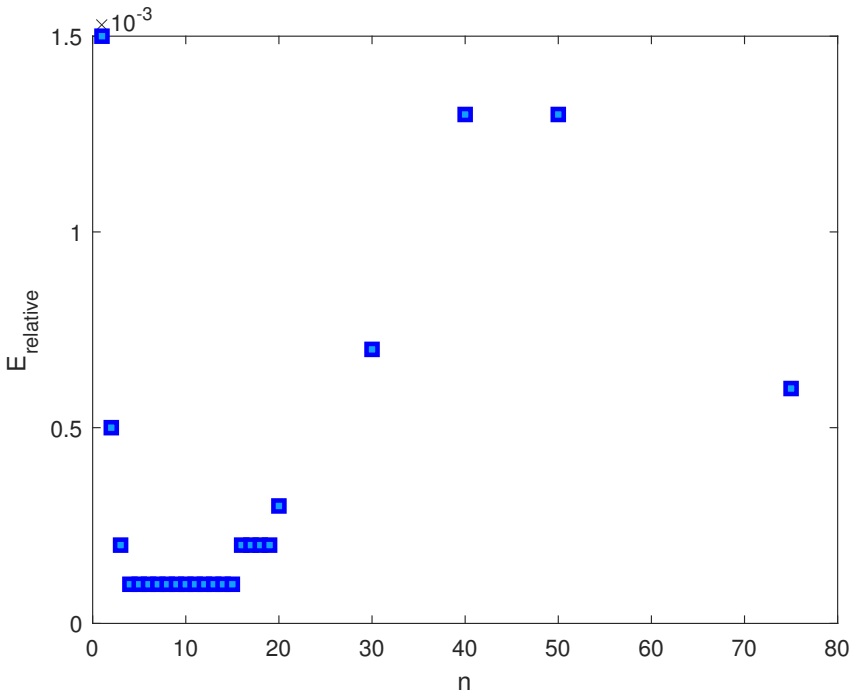

Figure 1. Relative errors for the symmetric potential $q(x) = |x(1-x)| - \frac{1}{6}$.

Example 2.

$$\left.\begin{array}{c} y''(x) + [\lambda^2 - \sin(|1-x|) + 1 - \cos 1]y(x) = 0, \quad 0 \le x \le 2 \\ y(0) + y'(0) = 0, \\ 0.5y(2) + \left(\dfrac{\sqrt{3}}{2} + 0.5\lambda\right)y'(2) = 0 \end{array}\right\} \tag{4.4}$$

In the second example, the potential function is treated as $q(x) = \sin(|1-x|) - 1 + \cos 1$. It is symmetric and integrable on $[0, 2]$. However, note that it is not continuous at midpoint 1. For this example, we choose $\gamma = \pi/2$, $\alpha = \pi/4$, $\beta = \pi/3$, and $c = 0.5$ in (1.1)–(1.3), and we have problem (4.4). Hence, with Theorem 2.2, the following asymptotic approximations for the eigenvalues of (4.4) are determined:

$$\lambda_n = \frac{(n+1)\pi}{2} + \frac{2}{(n+1)\pi}\left[-1 + \frac{\cos(n\pi) + \cos 1}{(n+1)^2\pi^2 - 1}\right] + O(n^{-1}\eta^2(n)) + O(n^{-2}\eta(n)). \tag{4.5}$$

For the selected parameter values, the asymptotic and numerical values, along with the resulting relative errors, are presented in Table 2.

As shown in Table 2, the asymptotic estimates are consistent with the numerical results. For the first 15 eigenvalues, the relative errors are generally on the order of 10^{-3}, while for the next 15 eigenvalues, they are on the order of 10^{-4}. For large eigenvalues, the errors increase to approximately 10^{-3}. The relative error plots for corresponding to the values of n are given in Figure 2.

From Figure 2, it is observed that while the initial relative errors are approximately on the order of 10^{-2}, the other eigenvalues exhibit much smaller error values.

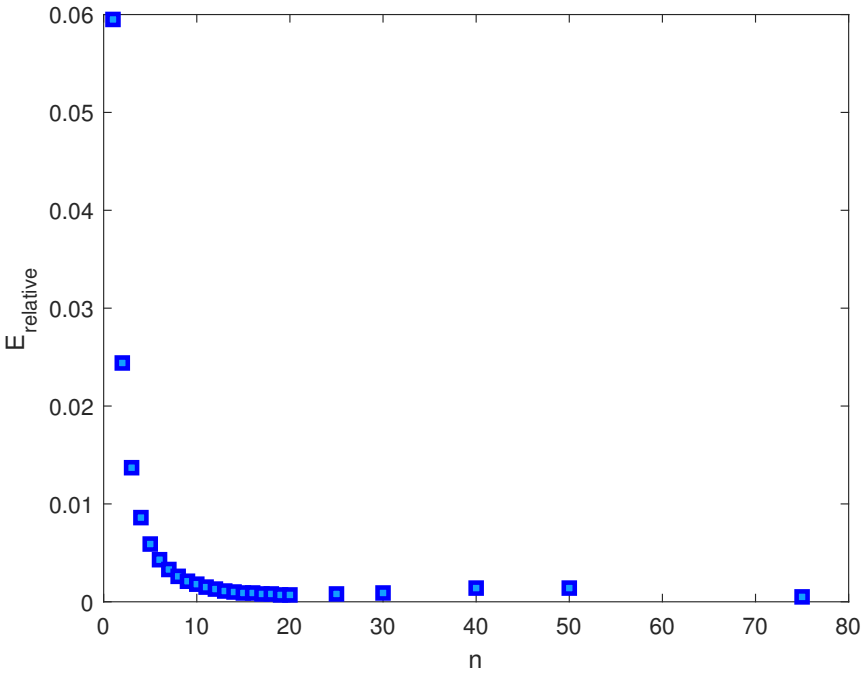

Figure 2. Relative errors for the symmetric potential $q(x) = \sin(|1-x|) - 1 + \cos 1$.

Table 2. Eigenvalue comparison for the symmetric potential $q(x) = \sin(|1 - x|) - 1 + \cos 1$.

n	Asymptotic Appr.	IEFG Appr.	Relative Error (E)
1	2.8195	2.9980	0.0595
2	4.5039	4.6167	0.0244
3	6.1236	6.2085	0.0137
4	7.7275	7.7942	0.0086
5	9.3185	9.3742	0.0059
6	10.9049	10.9523	0.0043
7	12.4867	12.5283	0.0033
8	14.0666	14.1035	0.0026
9	15.6443	15.6777	0.0021
10	17.2210	17.2515	0.0018
11	18.7965	18.8249	0.0015
12	20.3714	20.3980	0.0013
13	21.9457	21.9709	0.0011
14	23.5195	23.5437	0.0010
15	25.0929	25.1164	0.0009
16	26.6661	26.6891	0.0009
17	28.2390	28.2618	0.0008
18	29.8116	29.8345	0.0008
19	31.3841	31.4073	0.0007
20	32.9564	32.9802	0.0007
25	40.8162	40.8469	0.0008
30	48.6742	48.7190	0.0009
40	64.3871	64.4798	0.0014
50	80.0981	80.2113	0.0014
75	119.3721	119.3088	0.0005

5. Conclusions

In this paper, we aim to study the eigenvalues of a second-order boundary value problem in which the square root of the eigenvalue parameter appears in the boundary conditions, under the assumption that the potential function is integrable and symmetric on the given interval. We first seek the asymptotic eigenvalues of the problem, and then employ a numerical approach to verify the validity of the asymptotic results. In Section 2, we use the method improved by Harris in [21] for asymptotic approximation, and in Section 3, we deal with the IEFG method to find the eigenvalues numerically. The absence of a requirement to define a mesh between nodes provides a significant advantage for this method in solving differential equations. Furthermore, the approximation error of this method satisfies $\|u^h(x) - u(x)\|_{L^\infty(\Omega)} \leq c\|u^{m+1}\|_{L^\infty(\Omega)}\rho^{m+1}, u \in C^{m+1}(\Omega)$, where c is a constant and $\rho = \max_{1\leq i\leq N}\{\rho_i\}$ [34]. Since smaller values of ρ_i in the examples lead to smaller error values, it is demonstrated that the numerical results can be used to compare the accuracy of the asymptotic results.

In Section 3.1, we present the general forms of the shape functions and their derivatives obtained

via the IMLS method. Since the IEFG method relies on the weak form, the weak formulation of the problem is derived in Section 3.2. Choosing the shape functions as test functions, the system equation in (3.25) is obtained. From (3.25), it is observed that non-trivial solutions arise when the determinant of the coefficient matrix is zero. In (3.26), $F(\lambda)$ is defined as the determinant of the coefficient matrix in the system matrix. Therefore, the values that make this function zero correspond to the eigenvalues of the boundary value problem (1.1)–(1.3). In this study, the Newton–Raphson method is employed to compute the zeros of the function $F(\lambda)$.

In Section 4, two test problems are considered. The domain of the first problem is $[0, 1]$, whereas the second problem is defined on $[0, 2]$. For parameter values, the asymptotic and numerical results, along with the relative error values defined in the equation (4.1), are presented. In the numerical implementation, 100 nodal points are used for both problems. Tables 1 and 2 show that the numerical eigenvalues are consistent with the asymptotic eigenvalues. From Figures 1 and 2, the maximum relative error is observed to be on the order of 10^{-3} for the first problem and on the order of 10^{-2} for the second problem. The tables also indicate that the relative errors are generally on the order of 10^{-4} in the first problem, while in the second problem, they reach approximately 10^{-3} at some points. These results indicate that the error between the asymptotic and numerical approximations for the eigenvalues remains small in both problems.

Author contributions

All authors contributed equally to this work. All authors have accepted responsibility for the entire content of this manuscript and consented to its submission to the journal, reviewed all the results, and approved the final version of the manuscript.

Use of Generative-AI tools declaration

The authors declare that they have not used Artificial Intelligence (AI) tools in the creation of this article.

Acknowledgments

Both authors sincerely thank the referees for their insight and Recep Tayyip Erdoğan University for funding. This study has been supported by the Recep Tayyip Erdoğan University Development Foundation (Grant number: 02025012001837).

Conflict of interest

The authors declare no conflicts of interest.

References

1. A. Almalki, Sinc-galerkin method for Sturm–Liouville problem with applications in quantum mechanics, *J. Umm Al-Qura Univ. Appll. Sci.,* (2025), 1–11. https://doi.org/10.1007/s43994-025-00249-y

2. E. Başkaya, On the asymptotics of eigenvalues for a Sturm-Liouville problem with symmetric single-well potential, *Demonstr. Math.,* **57** (2024), 20230129. https://doi.org/10.1515/dema-2023-0129

3. E. Başkaya, On the gaps of Neumann eigenvalues for Hill's equation with symmetric double well potential, *Tbil. Math. J.,* **8** (2021), 139–145.

4. E. Başkaya, Periodic and semi-periodic eigenvalues of Hill's equation with symmetric double well potential, *TWMS J. Appl. Eng. Math.,* **10** (2020), 346–352. https://dergipark.org.tr/en/download/article-file/1181245

5. E. Baskaya, H. Coşkun, The derivative of spectral function of the problem with the boundary condition dependent on spectral parameter, *Turk. J. Math.,* **50** (2026), 153–163. https://doi.org/10.55730/1300-0098.3641

6. E. Başkaya, S. Şengül, On symmetric potential in a boundary value problem dependent on an eigenparameter, *AIMS Math.,* **10** (2025), 21835–21852. https://doi.org/10.3934/math.2025971

7. C. M. Bender, S. A. Orszag, *Advanced mathematical methods for scientists and engineers*, McGraw-Hill International Editions, 1987.

8. A. I. Benedek, R. Panzone, *On Sturm-Liouville Problems with the square-root of the eigenvalue parameter contained in the boundary conditions*, INMABB-CONICET, Universidad Nacional del Sur, 1981. https://www.inmabb-conicet.gob.ar/static/publicaciones/naa/naa-10.pdf

9. B. V. Brunt, *The calculus of variations*, Berlin: Springer, 2003.

10. N. M. Bujurke, C. S. Salimath, S. C. Shiralashetti, Computation of eigenvalues and solutions of regular Sturm–Liouville problems using Haar wavelets, *J. Comput. Appl. Math.,* **219** (2008), 90–101. https://doi.org/10.1016/j.cam.2007.07.005

11. Y. M. Cheng, F. N. Bai, M. J. Peng, A novel interpolating element-free Galerkin (IEFG) method for two-dimensional elastoplasticity, *Appl. Math. Model.,* **38** (2014), 5187–5197. https://doi.org/10.1016/j.apm.2014.04.008

12. I. Celik, Approximate calculation of eigenvalues with the method of weighted residuals–collocation method, *Appl. Math. Comput.,* **160** (2005), 401–410. https://doi.org/10.1016/j.amc.2003.11.011

13. B. Chanane, Computation of the eigenvalues of Sturm-Liouville problems with parameter dependent boundary conditions using the regularized sampling method, *Math. Comput.,* **74** (2005), 1793–1801. https://www.jstor.org/stable/4100211

14. B. Chanane, Computing the spectrum of non-self-adjoint Sturm–Liouville problems with parameter-dependent boundary conditions, *J. Comput. Appl. Math.,* **206** (2007), 229–237. https://doi.org/10.1016/j.cam.2006.06.014

15. H. Coşkun, E. Başkaya, A. Kabataş, Instability Intervals for Hill's equation with symmetric single well potential, *Ukr. Math. J.,* **71** (2019), 977–983. https://doi.org/10.1007/s11253-019-01692-x

16. H. Coşkun, A. Kabataş, E. Başkaya, On Green's function for boundary value problem with eigenvalue dependent quadratic boundary condition, *Bound. Value Probl.,* **2017** (2017), 71. https://doi.org/10.1186/s13661-017-0802-0

17. H. Coşkun, A. Kabataş, Asymptotic approximations of eigenfunctions for regular Sturm-Liouville Problems with eigenvalue parameter in the boundary condition for integrable potential, *Math. Scand.,* **113** (2013), 143–160. https://doi.org/10.7146/math.scand.a-15486

18. H. Coşkun, E. Başkaya, Asymptotics of eigenvalues of regular Sturm-Liouville problems with eigenvalue parameter in the boundary condition for integrable potential, *Math. Scand.,* **107** (2010), 209–223. https://doi.org/10.7146/math.scand.a-15152

19. Y. M. Frederick Wan, *Introduction to the calculus of variations and its applications*, London: Chapman and Hall, 1995. https://doi.org/10.1201/9780203749821

20. C. T. Fulton, Two point boundary value problems with eigenvalue parameter contained in the boundary conditions, *Proc. R. Soc. Edinb. A: Math.,* **77** (1977), 293–308. https://doi.org/10.1017/S030821050002521X

21. B. J. Harris, The form of the spectral functions associated with Sturm-Liouville problems with continuous spectrum, *Mathematika,* **44** (1997), 149–161. https://doi.org/10.1112/S0025579300012043

22. H. Hochstadt, On inverse problems associated with second-order differential operators, *Acta Math.,* **119** (1967), 173–192. https://doi.org/10.1007/BF02392082

23. A. Kabataş, Sturm-Liouville problems with non-linear dependence on the spectral parameter in the boundary conditions, *Bound. Value Probl.,* **118** (2025). https://doi.org/10.1186/s13661-025-02086-8

24. A. Kabataş, One boundary value problem including a spectral parameter in all boundary conditions, *Opusc. Math.,* **43** (2023), 651–661. https://doi.org/10.7494/OpMath.2023.43.5.651

25. A. Kabataş, Eigenfunction and Green's function asymptotics for Hill's equation with symmetric single well potential, *Ukr. Math. J.,* **74** (2022), 218–231. https://doi.org/10.37863/umzh.v74i2.6246

26. A. Kabataş, On eigenfunctions of Hill's equation with symmetric double well potential, *Commun. Fac. Sci. Univ. Ank. Ser. A1 Math. Stat.,* **71** (2022), 634–649. https://doi.org/10.31801/cfsuasmas.974409

27. N. B. Kerimov, K. R. Mamedov, On one boundary value problem with a spectral parameter in the boundary conditions, *Sib. Math. J.,* **40** (1999), 281–290. https://doi.org/10.1007/s11202-999-0008-5

28. P. Lancaster, K. Salkauskas, Surfaces generated by moving least squares methods, *Math. Comput.,* **37** (1981), 141–158. http://dx.doi.org/10.1090/S0025-5718-1981-0616367-1

29. O. S. Mukhtarov, M. Yücel, A study of the eigenfunctions of the singular Sturm–Liouville problem using the analytical method and the decomposition technique, *Mathematics,* **8** (2020), 415. https://doi.org/10.3390/math8030415

30. S. Y. Reutskiy, A meshless method for nonlinear, singular and generalized Sturm-Liouville problems, *Comput. Model. Eng. Sci.,* **34** (2008), 227. https://doi.org/10.3970/cmes.2008.034.227

31. Q. Shen, Numerical solution of the Sturm–Liouville problem with local RBF-based differential quadrature collocation method, *Int. J. Comput. Math.,* **88** (2011), 285–295. https://doi.org/10.1080/00207160903370180

32. M. M. Tharwat, H. B. Ali, Y. Ahmet, Numerical computation of eigenvalues of discontinuous Sturm–Liouville problems with parameter dependent boundary conditions using sinc method, *Numer. Algorithms,* **63** (2013), 27–48. https://doi.org/10.1007/s11075-012-9609-3

33. M. M. Tharwat, H. B. Ali, S. A. Abdulaziz, Approximation of eigenvalues of discontinuous Sturm-Liouville problems with eigenparameter in all boundary conditions, *Bound. Value Probl.,* **1** (2013), 132. https://doi.org/10.1186/1687-2770-2013-132

34. J. F. Wang, F. X. Sun, Y. M. Cheng,, A. X. Huang, Error estimates for the interpolating moving least-squares method, *Appl. Math. Comput.,* **245** (2014), 321–342. https://doi.org/10.1016/j.amc.2014.07.072

35. X. Yang, Z. Zhang, Analysis of a new NFV scheme preserving DMP for two-dimensional sub-diffusion equation on distorted meshes, *J. Sci. Comput.,* **99** (2024), 80. https://doi.org/10.1007/s10915-024-02511-7

36. X. Yang, Z. Zhang, Superconvergence analysis of a robust orthogonal Gauss collocation method for 2D fourth-order subdiffusion equations, *J. Sci. Comput.,* **100** (2024), 62. https://doi.org/10.1007/s10915-024-02616-z

37. J. Zhang, X. Yang, S. Wang, A compact difference method for the 2-D Kuramoto-Tsuzuki complex equation with Neumann boundary characterized by strong nonlinear effects, *Comput. Math. Appl.,* **203** (2026), 1–19. https://doi.org/10.1016/j.camwa.2025.11.013

38. Z. Zhang, X. Yang, Error estimation of α_p-robust ADI difference scheme on graded meshes for the three-dimensional nonlinear multiterm subdiffusion equation with constant coefficients, *Comput. Appl. Math.,* **45** (2026), 187. https://doi.org/10.1007/s40314-025-03469-4

AIMS Press